Vol. 4, No. 1, 2026
DOI: 10.61975/gjset.v4i1.105

ORIGINAL ARTICLE

Mechanistic Exploration of *Moringa oleifera Leaf Bioactives in Prostate Cancer Using Network Pharmacology*

Feniea Wulan Agaype Tengke[1], Trina Ekawati Tallei[2,3,*], Grace Lendawati Amelia Turalaki[2], Lydia Estelina Naomi Tendean[2], Martha Marie Kaseke[4], Nurdjannah Jane Niode[5], and Fatimawali Fatimawali[6,7]

[1]Medical Education Study Program, Faculty of Medicine, Sam Ratulangi University, Manado 95115, Indonesia; [2]Department of Biology, Faculty of Medicine, Sam Ratulangi University, Manado 95115, Indonesia; [3]Department of Biology, Faculty of Mathematics and Natural Sciences, Sam Ratulangi University, Manado 95115, Indonesia; [4]Department of Anatomy and Histology, Faculty of Medicine, Sam Ratulangi University, Manado 95115, Indonesia; [5]Department of Dermatology and Venereology, Faculty of Medicine, Sam Ratulangi University, Manado 95115, Indonesia; [6]Department of Chemistry, Faculty of Medicine, Sam Ratulangi University, Manado 95115, Indonesia; [7]Pharmacy Study Program, Faculty of Mathematics and Natural Sciences, Sam Ratulangi University, Manado 95115, Indonesia

* Correspondence: trina_tallei@unsrat.ac.id

Article History

Received
23 December 2026

Accepted
7 April 2026

Available Online
14 April 2026

Keywords

Network pharmacology
Moringa oleifera
Prostate cancer
In silico
ESR1
AKT1

Abstract

Prostate cancer remains one of the most prevalent malignancies in men worldwide, while current therapeutic strategies are often associated with adverse effects and the emergence of drug resistance, highlighting the need for safer and more effective alternatives. This study aimed to elucidate the multitarget molecular mechanisms of bioactive compounds derived from *Moringa oleifera* leaves against prostate cancer using an integrated *in silico* network pharmacology approach. A total of 137 bioactive compounds were collected from LC–MS/MS profiling data and phytochemical databases, of which 20 compounds with high predicted biological activity were prioritized based on Way2Drug PASS analysis. Potential protein targets were predicted and intersected with prostate cancer–associated genes to identify shared targets. Protein–protein interaction network analysis revealed 536 overlapping targets, with ten hub proteins, ESR1, AKT1, SRC, EGFR, TP53, HSP90AA1, PIK3CA, HSP90AB1, PIK3R1, and MAPK1, identified as central nodes. Pathway enrichment analysis demonstrated that these targets were predominantly involved in cancer-related signaling pathways, including pathways associated with EGFR tyrosine kinase inhibitor resistance. Pharmacokinetic and toxicity assessments indicated that several compounds, such as isorhamnetin, kaempferol, tocopherol, and afzelin, exhibited favorable drug-likeness properties and low predicted toxicity. Overall, these findings suggest that bioactive compounds from *Moringa oleifera* leaves exert anticancer effects through a multitarget and multi pathway mode of action rather than single-protein modulation. This study provides systematic insight into the molecular mechanisms underlying the anti–prostate cancer potential of *Moringa oleifera* leaves and supports their relevance as candidates for further experimental validation and drug development.

Introduction

Prostate cancer is among the most prevalent malignant tumors affecting men and remains a leading contributor to cancer-related mortality worldwide [1]. According to the Global Cancer Observatory (GLOBOCAN) 2022, prostate cancer ranks fourth globally, with approximately 1,466,680 new cases and an estimated 396,000 death [2]. In Indonesia, prostate cancer ranked eleventh among all cancer types in 2022, accounting for 13,130 newly diagnosed cases and approximately 4,860 deaths [3].

The initiation and early progression of prostate cancer are frequently associated with chronic inflammation of the prostate gland, which induces persistent cellular stress and DNA damage.

Sustained inflammatory activity promotes excessive production of reactive oxygen species (ROS), resulting in impaired DNA repair capacity and the accumulation of genetic mutations. Over time, this failure of DNA repair, together with inflammation-associated physiological alterations, contributes to genomic instability and facilitates malignant transformation [4].

Current therapeutic strategies for prostate cancer are determined by tumor characteristics, prostate-specific antigen (PSA) levels, disease stage and grade, and the risk of recurrence [1,5]. Available treatment modalities include active surveillance, surgical intervention, radiotherapy, hormone therapy, and chemotherapy [1,6]. However, these approaches are often accompanied by significant adverse effects, such as fatigue, alopecia, anorexia, erectile dysfunction, and urinary incontinence, which can substantially affect patients' quality of life. Consequently, there is a pressing need to develop safer therapeutic options with fewer side effects [7].

Natural products have long been recognized as valuable sources of bioactive compounds with anticancer potential, and medicinal plants play an important role in the development of alternative therapeutic strategies [8]. Among these, *Moringa oleifera* has attracted considerable attention as a promising anticancer agent [9]. Although all parts of the plant, including roots, leaves, flowers, and seeds exhibit therapeutic potential, *Moringa oleifera* leaves are the most extensively investigated due to their abundant bioactive constituents, such as flavonoids, alkaloids, and phenolic compounds [9,10]. Previous studies have demonstrated that glucomoringin isothiocyanate (GMG-ITC), derived from *Moringa oleifera* seeds, exerts cytotoxic effects on prostate cancer cells (PC-3) by inducing G2/M cell cycle arrest and activating the intrinsic, caspase-dependent mitochondrial apoptotic pathway [8]. *Moringa oleifera* leaf extract has been shown to exert antiproliferative and apoptosis-inducing effects on PC-3 prostate cancer cells through downregulation of the Hedgehog signaling pathway, while flower extract has been reported to induce cell cycle arrest and apoptosis via modulation of the AKT pathway [11,12]. In addition, alkaloids derived from *Moringa oleifera* have demonstrated inhibitory effects on PC-3 cell proliferation and migration through suppression of COX-2–mediated Wnt/β-catenin signaling, and specific compounds such as glucomoringin isothiocyanate have been shown to activate apoptotic pathways involving p53 and Akt/MAPK signaling [13].

Despite previous studies, the multitarget molecular mechanisms of *Moringa oleifera* bioactive compounds in prostate cancer remain insufficiently explored. Noor et al. [14] provided a general overview of network pharmacology applications without focusing on specific plant–disease interactions, while Okpako et al. [7] combined network pharmacology with molecular docking and in vitro validation on a different medicinal plant (*Aspilia pluriseta*). In contrast, the present study employs an integrated in silico network pharmacology approach specifically targeting *Moringa oleifera* leaves, prioritizing bioactive compounds based on TP53 upregulation, constructing high-confidence protein–protein interaction networks (STRING confidence score = 0.900), identifying hub proteins using multiple topological parameters, and evaluating pharmacokinetic and toxicity profiles. Accordingly, this study aims to identify bioactive compounds from *Moringa oleifera* leaves with potential relevance to prostate cancer, predict key protein targets and hub proteins using network pharmacology and protein–protein interaction analysis, elucidate associated signaling pathways, and evaluate the pharmacokinetic and toxicity profiles of prioritized compounds.

Materials and Methods

Bioactive Compound Profiling of Moringa oleifera Leaves

Information on bioactive compounds from *Moringa oleifera* leaves was obtained through a systematic literature search using the keywords "*Moringa oleifera* leaves," "bioactive compounds," and "network pharmacology," complemented by data retrieval from databases

such as Coconut (https://coconut.naturalproducts.net/) and Dr. Duke's Phytochemical and Ethnobotanical Databases (https://phytochem.nal.usda.gov/).

Compound Structure Profiling

The bioactive compounds of *Moringa oleifera* Leaves were profiled using the Simplified Molecular-Input Line-Entry System (SMILES) data retrieved from PubChem (https://pubchem.ncbi.nlm.nih.gov/).

Prediction of Bioactive Compound Activities from Moringa oleifera Leaves

The anticancer potential of bioactive compounds derived from *Moringa oleifera* leaves, particularly against prostate cancer, was predicted using WAY2DRUG PASS (https://www.way2drug.com/passonline/predict.php), which provides two probability estimates: probability to be active (Pa) and probability to be inactive (Pi). Predicted biological activities with Pa values greater than Pi were considered biologically plausible, indicating a higher likelihood of activity than inactivity [15]. Compounds with Pa ≥ 0.7 were classified as having a high probability of exhibiting biological activity, with a greater likelihood of experimental validation. Compounds with Pa values between 0.3 and 0.7 were considered to have moderate predicted activity, indicating potential biological relevance but with lower confidence and limited experimental support. In contrast, compounds with Pa ≤ 0.3 were regarded as having low predicted biological activity and a minimal likelihood of experimental validation [16,17].

Protein Target Identification and Analysis

The identification and analysis of protein targets associated with bioactive compounds from *Moringa oleifera* leaves were conducted using in silico computational prediction tools, including SwissTargetPrediction (http://www.swisstargetprediction.ch/) and the Similarity Ensemble Approach (SEA) (https://sea.bkslab.org/search). All predicted targets generated by SwissTargetPrediction and the Similarity Ensemble Approach (SEA) were initially included without applying an additional probability or confidence score threshold. Target predictions were restricted to *Homo sapiens*, and duplicate targets arising from overlap between the two platforms were removed to generate a non-redundant compound-associated target dataset prior to overlap analysis with prostate cancer–related genes. Proteins associated with prostate cancer were retrieved from GeneCards (https://www.genecards.org), GEPIA2 (http://gepia2.cancer-pku.cn/#index), and the Online Mendelian Inheritance in Man (OMIM) database (https://www.omim.org). From Genecards, all genes annotated as being associated with prostate cancer were collected without applying a relevance score cut-off. From GEPIA2, statistically significant differentially expressed genes were selected using the criteria $p<0.01$ and $|\log2 \text{ fold change}| > 1$. From OMIM, only genes explicitly annotated as being associated with prostate cancer were included. All prostate cancer–associated genes retrieved from GeneCards, GEPIA2, and OMIM were combined into a single dataset. Duplicate genes arising from overlap between databases were removed to generate a non-redundant gene set for subsequent analyses. Subsequently, targets associated with the bioactive compounds and those implicated in prostate cancer were mapped using the Draw Venn Diagram tool (https://bioinformatics.psb.ugent.be/webtools/Venn/) to identify overlapping targets. These shared targets were then subjected to functional annotation using ShinyGO version 0.82 (https://bioinformatics.sdstate.edu/go/), with a focus on biological processes and molecular pathways based on the Kyoto Encyclopedia of Genes and Genomes (KEGG) database.

Network Pharmacology Analysis

Protein–protein interaction (PPI) networks of the overlapping target proteins were constructed using the STRING database (version 12.0), with *Homo sapiens* specified as the reference organism. A minimum interaction confidence score of 0.900 (highest confidence) was applied. A full STRING network was employed, and all available interaction sources were enabled, including experimental evidence, curated databases, co-expression, gene neighborhood, gene

fusion, co-occurrence, and text mining. This analysis was conducted to characterize the functional associations and interaction patterns among the identified targets.

The resulting PPI network data were exported in TSV format and subsequently imported into Cytoscape (version 3.10.3) for network visualization, topological analysis, and further interpretation. Hub protein identification was performed using the Cytohubba plugin in Cytoscape. Network topology parameters, including degree, betweenness centrality, and closeness centrality, were applied to identify key proteins within the network. Proteins were ranked based on degree centrality, and the top 10 proteins with the highest degree values were defined as hub proteins. Betweenness and closeness centrality were used as supporting metrics to validate the central roles of these hub proteins.

Pharmacokinetic and Toxicity Evaluation

This study employed ADMET (Absorption, Distribution, Metabolism, Excretion, and Toxicity) parameters to evaluate the potential of compounds in new drug development, particularly with respect to their pharmacokinetic and toxicological properties. Lipinski's Rule of Five (Ro5) was used as a reference to assess the drug-likeness characteristics of each ligand. The SMILES notation was used as input data and analyzed using ADMETLab 3.0 (https://admetlab3.scbdd.com/server/evaluation) and ProTox 3.0 (https://tox.charite.de/protox3/index.php?site=compound_input) [18].

Results and Discussion

Bioactive Compound Profiling of Moringa oleifera Leaves

To ensure data consistency and avoid redundancy, the list of 137 bioactive compounds was compiled primarily from the comprehensive LC–MS/MS profiling study of *Moringa oleifera* leaves reported by Wang et al. [19], and complemented with data retrieved from public databases, including COCONUT and Dr. Duke's Phytochemical and Ethnobotanical Databases. In the study by Wang et al. [19], diverse classes of phytochemicals were identified, including phenolic acids, flavonoids, isothiocyanates, nucleosides, and alkaloids, highlighting the chemical complexity of *Moringa oleifera* leaves. The complete SMILES dataset of Moringa oleifera leaf compounds is provided in Table 1. Prior to downstream analysis, duplicate entries arising from overlapping database records or synonymous compound names were removed by cross-checking compound names and available chemical identifiers. When stereoisomeric forms were reported, compounds were treated as a single parent structure due to the lack of consistent stereochemical annotation across data sources. Compounds with incomplete structural information or ambiguous identifiers were excluded from subsequent target prediction analyses. It should also be noted that the compound profiling in this study relies on previously published LC–MS/MS data rather than de novo experimental analysis. As generally recognized in phytochemical and metabolomics research, variability in plant source, environmental conditions, extraction methods, and analytical parameters may influence phytochemical composition, which represents a limitation of the present study.

Table 1. Bioactive compounds of *Moringa oleifera* leaves and SMILES notation.

Code	Compound Name	SMILES
C1	Kaempferol	O=C1C(O)=C(C2=CC=C(O)C=C2)OC2=CC(O)=CC(O)=C12
C2	Zeaxanthin	CC1=C(/C=C/C(C)=C/C=C/C(C)=C/C=C/C=C(C)/C=C/C=C(C)/C=C/C2=C(C)C[C@@H](O)CC2(C)C)C(C)(C)C[C@H](O)C1
C3	Myrcene	C=CC(=C)CCC=C(C)C
C4	L-methionine	CSCC[C@H](N)C(=O)O

Code	Compound Name	SMILES
C5	Astragalin	O=C1C(O[C@@H]2O[C@H](CO)[C@@H](O)[C@H](O)[C@H]2O)=C(C2=CC=C(O)C=C2)OC2=CC(O)=CC(O)=C12
C6	Beta-Sitosterol	CC[C@H](CC[C@@H](C)[C@H]1CC[C@H]2[C@@H]3CC=C4C[C@@H](O)CC[C@]4(C)[C@H]3CC[C@]12C)C(C)C
C7	Benzylamine	NCC1=CC=CC=C1
C8	Afzelin	C[C@@H]1O[C@@H](OC2=C(C3=CC=C(O)C=C3)OC3=CC(O)=CC(O)=C3C2=O)[C@H](O)[C@H](O)[C@H]1O
C9	Ursolic acid	C[C@H]1[C@H](C)CC[C@]2(C(=O)O)CC[C@]3(C)C(=CC[C@@H]4[C@@]5(C)CC[C@H](O)C(C)(C)[C@@H]5CC[C@]43C)[C@H]12
C10	Hesperidin	COC1=CC=C([C@@H]2CC(=O)C3=C(O)C=C(O[C@@H]4O[C@H](CO[C@@H]5O[C@@H](C)[C@H](O)[C@@H](O)[C@H]5O)[C@@H](O)[C@H](O)[C@H]4O)C=C3O2)C=C1O
C11	L-glutamic acid	N[C@@H](CCC(=O)O)C(=O)O
C12	[(2S,3R,4R,5R,6S)-4,5-dihydroxy-2-[4-(isothiocyanatomethyl)phenoxy]-6-methyloxan-3-yl] acetate	CC(=O)O[C@H]1[C@H](OC2=CC=C(CN=C=S)C=C2)O[C@@H](C)[C@H](O)[C@H]1O
C13	kaempferol 3-O-[beta-glucosyl-(1→2)]-[alpha-rhamnosyl-(1→6)]-beta-glucoside-7-O-alpha-rhamnoside	C[C@H]1OC(OC[C@H]2OC(OC3=C(C4=CC=C(O)C=C4)OC4=CC(OC5O[C@H](C)[C@@H](O)[C@H](O)[C@@H]5O)=CC(O)=C4C3=O)[C@@H](OC3O[C@H](CO)[C@@H](O)[C@H](O)[C@H]3O)[C@@H](O)[C@@H]2O)[C@@H](O)[C@@H](O)[C@@H]1O
C14	4-[(4'-O-Acetyl-alpha-L-rhamnosyloxy)benzyl]isothiocyanate	CC(=O)O[C@@H]1[C@@H](O)[C@@H](O)[C@H](OC2=CC=C(CN=C=S)C=C2)O[C@H]1C
C15	[(2S,3R,4R,5S,6S)-3,5-dihydroxy-2-[4-(isothiocyanatomethyl)phenoxy]-6-methyloxan-4-yl] acetate	CC(=O)O[C@@H]1[C@@H](O)[C@H](C)O[C@@H](OC2=CC=C(CN=C=S)C=C2)[C@@H]1O
C16	Narirutin	C[C@@H]1O[C@@H](OC[C@H]2O[C@@H](OC3=CC(O)=C4C(=O)C[C@@H](C5=CC=C(O)C=C5)OC4=C3)[C@H](O)[C@@H](O)[C@@H]2O)[C@H](O)[C@H](O)[C@H]1O
C17	Methyl 4-hydroxybenzoate	COC(=O)C1=CC=C(O)C=C1
C18	Lutein	CC1=C[C@H](O)CC(C)(C)[C@H]1/C=C/C(C)=C/C=C/C(C)=C/C=C/C=C(C)/C=C/C=C(C)/C=C/C1=C(C)C[C@@H](O)CC1(C)C
C19	kaempferol 3-O-[alpha-rhamnosyl-(1→2)]-[alpha-rhamnosyl-(1→4)]-beta-glucoside-7-O-alpha-rhamnoside	C[C@H]1OC(OC[C@H]2OC(OC3=C(C4=CC=C(O)C=C4)OC4=CC(OC5O[C@H](C)[C@@H](O)[C@H](O)[C@@H]5O)=CC(O)=C4C3=O)[C@@H](OC3O[C@H](C)[C@@H](O)[C@H](O)[C@H]3O)[C@@H](O)[C@@H]2O)[C@@H](O)[C@@H](O)[C@@H]1O
C20	Clausarin	C=CC(C)(C)C1=CC2=C(O)C3=C(OC(C)(C)C=C3)C(C(C)(C)C=C)=C2OC1=O
C21	L-histidine	N[C@@H](CC1=CN=CN1)C(=O)O
C22	Ascorbic Acid	O=C1O[C@H]([C@@H](O)CO)C(O)=C1O
C23	Asperglaucide	CC(=O)OC[C@H](CC1=CC=CC=C1)NC(=O)[C@H](CC1=CC=CC=C1)NC(=O)C1=CC=CC=C1
C24	Methyl vanillate	COC(=O)C1=CC=C(O)C(OC)=C1
C25	Arginine	N=C(N)NCCC[C@H](N)C(=O)O
C26	L-isoleucine	CC[C@H](C)[C@H](N)C(=O)O
C27	L-alanine	C[C@H](N)C(=O)O
C28	Myricetin	O=C1C(O)=C(C2=CC(O)=C(O)C(O)=C2)OC2=CC(O)=CC(O)=C12

Code	Compound Name	SMILES
C29	4-hydroxybenzoic acid	O=C(O)C1=CC=C(O)C=C1
C30	Kaempferide 3-O-(2''-O-galloylrutinoside)-7-O-alpha-rhamnoside	COC1=CC=C(C2=C(OC3O[C@H](C)[C@@H](O)[C@H](O)[C@@]3(O)C(=O)C3=CC(O)=C(O)C(O)=C3)C(=O)C3=C(O)C=C(OC4O[C@H](C)[C@@H](O)[C@H](O)[C@@H]4O)C=C3O2)C=C1
C31	Alpha-terpinene	CC1=CC=C(C(C)C)CC1
C32	Glucosinalbin	O=S(=O)(O)O/N=C(\CC1=CC=C(O)C=C1)S[C@@H]1O[C@H](CO)[C@@H](O)[C@H](O)[C@H]1O
C33	4-Hydroxybenzaldehyde rhamnoside	C[C@@H]1O[C@@H](OC2=CC=C(C=O)C=C2)[C@H](O)[C@H](O)[C@H]1O
C34	Ponfolin	C=CC(C)(C)OC1=C2C=CC(C)(C)OC2=C(C(C)(C)C=C)C2=C1C=CC(=O)O2
C35	7-hydroxy-6,8-bis(3-methylbut-2-enyl)chromen-2-one	CC(C)=CCC1=CC2=C(OC(=O)C=C2)C(CC=C(C)C)=C1O
C36	1,3-dibenzylurea	O=C(NCC1=CC=CC=C1)NCC1=CC=CC=C1
C37	Benzyl beta-primeveroside	O[C@@H]1[C@@H](O)[C@H](OCC2=CC=CC=C2)O[C@H](CO[C@@H]2OC[C@@H](O)[C@H](O)[C@H]2O)[C@H]1O
C38	Dentatin	C=CC(C)(C)C1=C2OC(C)(C)C=CC2=C(OC)C2=C1OC(=O)C=C2
C39	Sesamolin	C1=CC2=C(C=C1O[C@H]1OC[C@H]3[C@@H]1CO[C@@H]3C1=CC=C3OCOC3=C1)OCO2
C40	Junosidine	COC1=CC=CC2=C1N(C)C1=CC3=C(C=CC(C)(C)O3)C(O)=C1C2=O
C41	Niazimin	CCOC(=O)NCC1=CC=C(O[C@@H]2O[C@@H](C)[C@H](OC(C)=O)[C@@H](O)[C@H]2O)C=C1
C42	4-(4'-O-Acetyl-alpha-L-rhamnosyloxy)benzaldehyde	CC(=O)O[C@@H]1[C@@H](O)[C@@H](O)[C@H](OC2=CC=C(C=O)C=C2)O[C@H]1C
C43	[(2R,3R,4S,5R,6S)-3,4,5-trihydroxy-6-(hydroxymethyl)tetrahydropyran-2-yl] (1Z)-2-(4-hydroxyphenyl)-N-sulfooxy-ethanimidothioate	O=S(=O)(O)O/N=C(/CC1=CC=C(O)C=C1)S[C@H]1O[C@@H](CO)[C@H](O)[C@H](O)[C@H]1O
C44	Niazicinin A	COC(=O)NCC1=CC=C(O[C@@H]2O[C@@H](C)[C@H](OC(C)=O)[C@@H](O)[C@H]2O)C=C1
C45	Nomilin	CC(=O)O[C@H]1CC(=O)OC(C)(C)[C@@H]2CC(=O)[C@]3(C)[C@H](CC[C@@]4(C)[C@H](C5=COC=C5)OC(=O)[C@H]5O[C@]543)[C@@]12C
C46	Benzylcarbamic Acid	O=C(O)NCC1=CC=CC=C1
C47	4-(4'-O-Acetyl-alpha-L-rhamnopyranosyloxyl)benzyl glucosinolate	CC(=O)O[C@@H]1[C@H](O)[C@H](O)[C@H](OC2=CC=C(C/C(=N/OS(=O)(=O)O)S[C@H]3O[C@@H](CO)[C@@H](O)[C@@H](O)[C@H]3O)C=C2)O[C@H]1C
C48	Marumoside A	C[C@@H]1O[C@@H](OC2=CC=C(CC(N)=O)C=C2)[C@H](O)[C@H](O)[C@H]1O
C49	2-[4-[(2S,3R,4R,5S,6S)-3,5-dihydroxy-6-methyl-4-[(2S,3R,4S,5S,6R)-3,4,5-trihydroxy-6-(hydroxymethyl)tetrahydropyran-2-yl]oxy-tetrahydropyran-2-yl]oxyphenyl]acetamide	C[C@@H]1O[C@@H](OC2=CC=C(CC(N)=O)C=C2)[C@H](O)[C@H](O[C@@H]2O[C@H](CO)[C@@H](O)[C@H](O)[C@H]2O)[C@H]1O
C50	N-methoxycarbonyl-4-(alpha-l-rhamnopyranosyloxy) benzylamine	COC(=O)NCC1=CC=C(O[C@@H]2O[C@@H](C)[C@H](O)[C@@H](O)[C@H]2O)C=C1
C51	[(2R,3R,4R,5R,6R)-3,4,5-trihydroxy-6-(hydroxymethyl)tetrahydropyran-2-yl] (1Z,2R)-2-methyl-N-sulfooxy-butanimidothioate	CC[C@@H](C)/C(=N/OS(=O)(=O)O)S[C@H]1O[C@H](CO)[C@H](O)[C@@H](O)[C@H]1O
C52	[(2S,3R,4S,5R,6S)-6-[4-[[(Z)-(2-ethoxy-2-	CCOC(=S)/C=N\CC1=CC=C(O[C@@H]2O[C@@H](C)[C@H](OC(C)=O)[C@@H](O)[C@H]2O)C=C1

Code	Compound Name	SMILES
	sulfanylideneethylidene)amino]methyl]phenoxy]-4,5-dihydroxy-2-methyloxan-3-yl] acetate	
C53	Nomilinic Acid	CC(=O)O[C@H](CC(=O)O)[C@]1(C)[C@H]2CC[C@@]3(C)[C@H](C4=COC=C4)OC(=O)[C@H]4O[C@]43[C@]2(C)C(=O)C[C@H]1C(C)(C)O
C54	[(2S,3R,4S,5R,6S)-6-[4-[[(E)-(2-ethoxy-2-sulfanylideneethylidene)amino]methyl]phenoxy]-4,5-dihydroxy-2-methyloxan-3-yl] acetate	CCOC(=S)/C=N/CC1=CC=C(O[C@@H]2O[C@@H](C)[C@H](OC(C)=O)[C@@H](O)[C@H]2O)C=C1
C55	S-methyl N-[[4-[(2S,3R,4R,5R,6S)-3,4,5-trihydroxy-6-methyloxan-2-yl]oxyphenyl]methyl]carbamothioate	CSC(=O)NCC1=CC=C(O[C@@H]2O[C@@H](C)[C@H](O)[C@@H](O)[C@H]2O)C=C1
C56	Ethyl 4-(rhamnosyloxy)benzylcarbamate	CCOC(=O)NCC1=CC=C(O[C@@H]2O[C@@H](C)[C@H](O)[C@@H](O)[C@H]2O)C=C1
C57	Cyanidin 3-(6''-acetyl-galactoside)	CC(=O)OC[C@H]1O[C@@H](OC2=CC3=C(O)C=C(O)C=C3[O+]=C2C2=CC=C(O)C(O)=C2)[C@H](O)[C@@H](O)[C@H]1O
C58	[(2R,3R,4S,5R,6S)-3,4,5-trihydroxy-6-(hydroxymethyl)tetrahydropyran-2-yl] (1Z)-2-methyl-N-sulfooxy-propanimidothioate	CC(C)/C(=N/OS(=O)(=O)O)S[C@H]1O[C@@H](CO)[C@H](O)[C@H](O)[C@H]1O
C59	4-Hydroxyphenylacetonitrile triacetylrhamnoside	CC(=O)O[C@@H]1[C@@H](OC(C)=O)[C@H](C)O[C@@H](OC2=CC=C(CC#N)C=C2)[C@@H]1OC(C)=O
C60	[(2R,3R,4S,5R,6S)-3,4,5-trihydroxy-6-(hydroxymethyl)tetrahydropyran-2-yl] (1Z)-N-sulfooxy-2-[4-[(2S,3R,4S,5R,6S)-3,4,5-trihydroxy-6-methyl-tetrahydropyran-2-yl]oxyphenyl]ethanimidothioate	C[C@@H]1O[C@@H](OC2=CC=C(C/C(=N/OS(=O)(=O)O)S[C@H]3O[C@@H](CO)[C@H](O)[C@H](O)[C@H]3O)C=C2)[C@H](O)[C@@H](O)[C@H]1O
C61	(1R)-1-isopropenyl-4-methyl-cyclohex-3-en-1-ol	C=C(C)[C@]1(O)CC=C(C)CC1
C62	1-ethoxy-N-[[4-[(2S,3R,4R,5R,6S)-3,4,5-trihydroxy-6-methyloxan-2-yl]oxyphenyl]methyl]methanimidothioic acid	CCOC(S)=NCC1=CC=C(O[C@@H]2O[C@@H](C)[C@H](O)[C@@H](O)[C@H]2O)C=C1
C63	(3R,5R)-4-[3-(3,4-dihydroxyphenyl)prop-2-enoyloxy]-1,3,5-trihydroxy-cyclohexanecarboxylic acid	O=C(C=CC1=CC=C(O)C(O)=C1)O[C@H]1[C@H](O)C[C@](O)(C(=O)O)C[C@H]1O
C64	2-[3-hydroxy-4-[(2R,3R,4R,5R,6S)-3,4,5-trihydroxy-6-methyl-tetrahydropyran-2-yl]oxy-phenyl]acetonitrile	C[C@@H]1O[C@H](OC2=CC=C(CC#N)C=C2O)[C@H](O)[C@H](O)[C@H]1O
C65	[(2S,3R,4S,5S,6R)-3,4,5-trihydroxy-6-(hydroxymethyl)oxan-2-yl] (1Z)-N-sulfooxy-2-[4-[(2R,3S,4S,5S,6R)-3,4,5-trihydroxy-6-methyloxan-2-yl]oxyphenyl]ethanimidothioate	C[C@H]1O[C@H](OC2=CC=C(C/C(=N/OS(=O)(=O)O)S[C@@H]3O[C@H](CO)[C@@H](O)[C@H](O)[C@H]3O)C=C2)[C@@H](O)[C@@H](O)[C@@H]1O
C66	(3R)-5-[[(2R,3S,4S,5R,6S)-6-[2-(3,4-dihydroxyphenyl)-5,7-dihydroxy-4-oxo-chromen-3-yl]oxy-3,4,5-trihydroxy-tetrahydropyran-2-yl]methoxy]-3-	C[C@@](O)(CC(=O)O)CC(=O)OC[C@H]1O[C@@H](OC2=C(C3=CC=C(O)C(O)=C3)OC3=CC(O)=CC(O)=C3C2=O)[C@H](O)[C@@H](O)[C@@H]1O

Code	Compound Name	SMILES
	hydroxy-3-methyl-5-oxo-pentanoic acid	
C67	(2R,3S,4S,5R,6R)-2-methyl-6-phenoxy-tetrahydropyran-3,4,5-triol	C[C@H]1O[C@H](OC2=CC=CC=C2)[C@H](O)[C@@H](O)[C@@H]1O
C68	[(2R,3S,4R,5R,6R)-4,5-dihydroxy-6-[4-[(methoxycarbonylamino)methyl]phenoxy]-2-methyl-tetrahydropyran-3-yl] acetate	COC(=O)NCC1=CC=C(O[C@H]2O[C@H](C)[C@@H](OC(C)=O)[C@H](O)[C@H]2O)C=C1
C69	1-[(2R,3R,4S,5S,6R)-3,4,5-trihydroxy-6-(hydroxymethyl)oxan-2-yl]oxy-N-[[4-[(2S,3R,4S,5S,6R)-3,4,5-trihydroxy-6-methyloxan-2-yl]oxyphenyl]methyl]methanimidothioic acid	C[C@H]1O[C@@H](OC2=CC=C(CN=C(S)O[C@H]3O[C@H](CO)[C@@H](O)[C@H](O)[C@H]3O)C=C2)[C@H](O)[C@@H](O)[C@@H]1O
C70	2-[4-[(2R,3R,4S,5R,6R)-3,5-dihydroxy-6-methyl-4-[(2S,3R,4S,5S,6R)-3,4,5-trihydroxy-6-(hydroxymethyl)tetrahydropyran-2-yl]oxy-tetrahydropyran-2-yl]oxyphenyl]acetonitrile	C[C@H]1O[C@H](OC2=CC=C(CC#N)C=C2)[C@H](O)[C@@H](O[C@@H]2O[C@H](CO)[C@@H](O)[C@H](O)[C@H]2O)[C@@H]1O
C71	[(2S,3R,4S,5R,6S)-6-[4-[[[ethoxy(sulfanyl)methylidene]amino]methyl]phenoxy]-4,5-dihydroxy-2-methyloxan-3-yl] acetate	CCOC(S)=NCC1=CC=C(O[C@@H]2O[C@@H](C)[C@H](OC(C)=O)[C@@H](O)[C@H]2O)C=C1
C72	(2R,3S,4S)-3-[(2S,3R,4R,5S,6R)-3,4-dihydroxy-6-(hydroxymethyl)-5-[(2S,3R,4S,5R,6R)-3,4,5-trihydroxy-6-(hydroxymethyl)tetrahydropyran-2-yl]oxy-tetrahydropyran-2-yl]oxy-2-(3,4,5-trihydroxyphenyl)chromane-4,5,7-triol	OC[C@H]1O[C@@H](O[C@H]2[C@H](O)[C@@H](O)[C@H](O[C@@H]3[C@@H](C4=CC(O)=C(O)C(O)=C4)OC4=CC(O)=CC(O)=C4[C@@H]3O)O[C@@H]2CO)[C@H](O)[C@@H](O)[C@H]1O
C73	(3R,5R)-1,3,5-trihydroxy-4-[(E)-3-[3-hydroxy-4-[(2R,3R,4S,5S,6R)-3,4,5-trihydroxy-6-(hydroxymethyl)tetrahydropyran-2-yl]oxy-phenyl]prop-2-enoyl]oxy-cyclohexanecarboxylic acid	O=C(/C=C/C1=CC=C(O[C@H]2O[C@H](CO)[C@@H](O)[C@H](O)[C@H]2O)C(O)=C1)O[C@H]1[C@H](O)C[C@](O)(C(=O)O)C[C@H]1O
C74	4-hydroxy-7,8-dimethyl-10-[(2S,3S,4R)-2,3,4,5-tetrahydroxypentyl]benzo[g]pteridin-2-one	CC1=CC2=C(C=C1C)N(C[C@H](O)[C@H](O)[C@H](O)CO)C1=NC(=O)N=C(O)C1=N2
C75	(2R,3R,4S,5S,6R)-2-benzyloxy-6-[[(2S,3S,4R,5R)-3,4,5-trihydroxytetrahydropyran-2-yl]oxymethyl]tetrahydropyran-3,4,5-triol	O[C@@H]1[C@@H](O)[C@H](OCC2=CC=CC=C2)O[C@H](CO[C@@H]2OC[C@@H](O)[C@@H](O)[C@@H]2O)[C@H]1O
C76	methyl 2-[4-[(2R,3R,4S,5S,6R)-3,4,5-trihydroxy-6-methyl-tetrahydropyran-2-yl]oxyphenyl]acetate	COC(=O)CC1=CC=C(O[C@H]2O[C@H](C)[C@@H](O)[C@H](O)[C@H]2O)C=C1
C77	(1R,2R,7S,10S,13R,14R,16S,19S,20S)-19-(3-furyl)-9,9,13,20-tetramethyl-4,8,15,18-tetraoxahexacyclo[11.9.0.0^{2,7}.0	CC1(C)O[C@H]2CC(=O)OC[C@@]23[C@@H]1CC(=O)[C@]1(C)[C@@H]3CC[C@@]2(C)[C@H](C3=COC=C3)OC(=O)[C@H]3O[C@]321

Code	Compound Name	SMILES
	^{2,10}.0^{14,16}.0^{14,20}]docosane-5,12,17-trione	
C78	(3R,8R,9R,10S,13R,14R,17S)-17-[(1R,4R)-4-ethyl-1,5-dimethyl-hexyl]-10,13-dimethyl-2,3,4,7,8,9,11,12,14,15,16,17-dodecahydro-1H-cyclopenta[a]phenanthren-3-ol	CC[C@H](CC[C@@H](C)[C@@H]1CC[C@@H]2[C@H]3CC=C4C[C@H](O)CC[C@@]4(C)[C@@H]3CC[C@@]21C)C(C)C
C79	[(2R,3S,4R,5R,6R)-4,5-dihydroxy-6-[4-[[[methoxy(sulfanyl)methylidene]amino]methyl]phenoxy]-2-methyloxan-3-yl] acetate	COC(S)=NCC1=CC=C(O[C@H]2O[C@H](C)[C@@H](OC(C)=O)[C@H](O)[C@H]2O)C=C1
C80	5-(hydroxymethyl)-1-[[4-[(2S,3R,4R,5R,6S)-3,4,5-trihydroxy-6-methyl-tetrahydropyran-2-yl]oxyphenyl]methyl]pyrrole-2-carbaldehyde	C[C@@H]1O[C@@H](OC2=CC=C(CN3C(C=O)=CC=C3CO)C=C2)[C@H](O)[C@H](O)[C@H]1O
C81	methyl N-[[4-[(2R,3R,4S,5S,6R)-3,4,5-trihydroxy-6-methyl-tetrahydropyran-2-yl]oxyphenyl]methyl]carbamate	COC(=O)NCC1=CC=C(O[C@H]2O[C@H](C)[C@@H](O)[C@H](O)[C@H]2O)C=C1
C82	[(2S,3S,4R,5R,6S)-4,5-diacetyloxy-6-[4-[[[ethoxy(sulfanyl)methylidene]amino]methyl]phenoxy]-2-methyloxan-3-yl] acetate	CCOC(S)=NCC1=CC=C(O[C@@H]2O[C@@H](C)[C@H](OC(C)=O)[C@@H](OC(C)=O)[C@H]2OC(C)=O)C=C1
C83	[(2S,3R,4S,5R,6S)-4,5-dihydroxy-6-[4-[[[methoxy(sulfanyl)methylidene]amino]methyl]phenoxy]-2-methyloxan-3-yl] acetate	COC(S)=NCC1=CC=C(O[C@@H]2O[C@@H](C)[C@H](OC(C)=O)[C@@H](O)[C@H]2O)C=C1
C84	2-[4-[(2R,3R,4S,5S,6R)-3,4,5-trihydroxy-6-methyl-tetrahydropyran-2-yl]oxyphenyl]acetonitrile	C[C@H]1O[C@H](OC2=CC=C(CC#N)C=C2)[C@H](O)[C@@H](O)[C@@H]1O
C85	(3R)-3-[(1R,2R,4S,7S,8S,11R,12R,16S)-7-(3-furyl)-1,8,15,15-tetramethyl-5,18-dioxo-3,6,14-trioxapentacyclo[9.7.0.0^{2,4}.0^{2,8}.0^{12,16}]octadecan-12-yl]-3-hydroxy-propanoic acid	CC1(C)OC[C@]2([C@H](O)CC(=O)O)[C@@H]1CC(=O)[C@]1(C)[C@@H]2CC[C@@]2(C)[C@H](C3=COC=C3)OC(=O)[C@H]3O[C@]321
C86	(3R,5R)-1,3,5-trihydroxy-4-[3-[4-hydroxy-3-[(2R,3R,4S,5S,6R)-3,4,5-trihydroxy-6-(hydroxymethyl)tetrahydropyran-2-yl]oxy-phenyl]prop-2-enoyloxy]cyclohexanecarboxylic acid	O=C(C=CC1=CC=C(O)C(O[C@H]2O[C@H](CO)[C@@H](O)[C@H](O)[C@H]2O)=C1)O[C@H]1[C@H](O)C[C@](O)(C(=O)O)C[C@H]1O
C87	(1R,2'S,3aR,5aR,6R,7S,9aR,9bR)-7-[(S)-3-furyl-[(2R,3R,4S,5S,6R)-3,4,5-trihydroxy-6-(hydroxymethyl)tetrahydropyran-2-yl]oxy-methyl]-1-hydroxy-1,3,3,5a,7,9b-hexamethyl-5-oxo-spiro[4,8,9,9a-tetrahydro-3aH-	CC1(C)O[C@@](C)(O)[C@]2(C)[C@H]3CC[C@@](C)([C@@H](O[C@@H]4O[C@H](CO)[C@@H](O)[C@H](O)[C@H]4O)C4=COC=C4)[C@@]4(O[C@@H]4C(=O)O)[C@]3(C)C(=O)C[C@@H]12

Code	Compound Name	SMILES
	benzo[e]isobenzofuran-6,3'-oxirane]-2'-carboxylic acid	
C88	1-cyanato-N-[[4-[(2S,3R,4R,5R,6S)-3,4,5-trihydroxy-6-methyloxan-2-yl]oxyphenyl]methyl]methanimidothioic acid	C[C@@H]1O[C@@H](OC2=CC=C(CN=C(S)OC#N)C=C2)[C@H](O)[C@H](O)[C@H]1O
C89	1-methoxy-N-[[4-[(2S,3R,4R,5R,6S)-3,4,5-trihydroxy-6-methyloxan-2-yl]oxyphenyl]methyl]methanimidothioic acid	COC(S)=NCC1=CC=C(O[C@@H]2O[C@@H](C)[C@H](O)[C@@H](O)[C@H]2O)C=C1
C90	2-[3-hydroxy-4-[(2S,3R,4R,5R,6S)-3,4,5-trihydroxy-6-methyl-tetrahydropyran-2-yl]oxy-phenyl]acetonitrile	C[C@@H]1O[C@@H](OC2=CC=C(CC#N)C=C2O)[C@H](O)[C@H](O)[C@H]1O
C91	Malic acid	C(C(C(=O)O)O)C(=O)O
C92	Trigonelline	C[N+]1=CC=CC(=C1)C(=O)[O-]
C93	5-Hydroxymethylfurfural	C1=C(OC(=C1)C=O)CO
C94	L-Valine	CC(C)[C@@H](C(=O)O)N
C95	Cytosine	C1=C(NC(=O)N=C1)N
C96	Benzaldehyde	C1=CC=C(C=C1)C=O
C97	Cinnamic acid	C1=CC=C(C=C1)/C=C/C(=O)O
C98	p-Coumaric acid	C1=CC(=CC=C1/C=C/C(=O)O)O
C99	Citric Acid	C(C(=O)O)C(CC(=O)O)(C(=O)O)O
C100	Cinnamaldehyde	C1=CC=C(C=C1)/C=C/C=O
C101	L-Leucine	CC(C)C[C@@H](C(=O)O)N
C102	Protocatechuic acid-4-O-glucoside	C1=CC(=C(C=C1C(=O)O)O)OC2C(C(C(C(O2)CO)O)O)O
C103	Salicylic acid	C1=CC=C(C(=C1)C(=O)O)O
C104	Nicotinamide	C1=CC(=CN=C1)C(=O)N
C105	Guanosine	C1=NC2=C(N1[C@H]3[C@@H]([C@@H]([C@H](O3)CO)O)O)N=C(NC2=O)N
C106	L-Phenylalanine	CN(C)[C@@H](CC1=CC=CC=C1)C(=O)O
C107	Gallic acid 4-O-glucoside	C1=C(C=C(C(=C1O)O[C@H]2[C@@H]([C@H]([C@@H]([C@H](O2)CO)O)O)O)O)C(=O)O
C108	Glucomoringin	C[C@H]1[C@@H]([C@H]([C@H]([C@@H](O1)OC2=CC=C(C=C2)C/C(=N\OS(=O)(=O)[O-])/S[C@H]3[C@@H]([C@H]([C@@H]([C@H](O3)CO)O)O)O)O)O)O.[K+]
C109	Adenosine	C1=NC(=C2C(=N1)N(C=N2)[C@H]3[C@@H]([C@@H]([C@H](O3)CO)O)O)N
C110	Gallic acid	C1=C(C=C(C(=C1O)O)O)C(=O)O
C111	Neochlorogenic acid	C1[C@H]([C@@H]([C@@H](C[C@]1(C(=O)O)O)OC(=O)/C=C/C2=CC(=C(C=C2)O)O)O)O
C112	Protocatechuic acid	C1=CC(=C(C=C1C(=O)O)O)O
C113	Chlorogenic acid	C1[C@H]([C@H]([C@@H](C[C@@]1(C(=O)O)O)OC(=O)/C=C/C2=CC(=C(C=C2)O)O)O)O
C114	Vicenin-2	C1=CC(=CC=C1C2=CC(=O)C3=C(C(=C(C(=C3O2)[C@H]4[C@@H]([C@H]([C@@H]([C@H](O4)CO)O)O)O)O)[C@H]5[C@@H]([C@H]([C@@H]([C@H](O5)CO)O)O)O)O)O
C115	7-Hydroxycoumarin	C1=CC(=CC2=C1C=CC(=O)O2)O
C116	p-Coumaroylquinic acid	C1[C@@H]([C@@H]([C@H](C[C@]1(C(=O)O)O)OC(=O)/C=C/C2=CC=C(C=C2)O)O)O
C117	Cryptochlorogenic acid	C1[C@H](C([C@@H](CC1(C(=O)O)O)O)OC(=O)/C=C/C2=CC(=C(C=C2)O)O)O

Code	Compound Name	SMILES
C118	Rutin	C[C@H]1[C@@H]([C@H]([C@H]([C@@H](O1)OC[C@@H]2[C@H]([C@@H]([C@H]([C@@H](O2)OC3=C(OC4=CC(=CC(=C4C3=O)O)O)C5=CC(=C(C=C5)O)O)O)O)O)O)O)O
C119	Protocatechualdehyde	C1=CC(=C(C=C1C=O)O)O
C120	3-O-Feruloylquinic acid	COC1=C(C=CC(=C1)/C=C/C(=O)O[C@@H]2C[C@@](C[C@H]([C@H]2O)O)(C(=O)O)O)O
C121	Vitexin	C1=CC(=CC=C1C2=CC(=O)C3=C(O2)C(=C(C=C3O)O)[C@H]4[C@@H]([C@H]([C@@H]([C@H](O4)CO)O)O)O)O
C122	Kaempferol-3-O-rutinoside	C[C@H]1[C@@H]([C@H]([C@H]([C@@H](O1)OC[C@@H]2[C@H]([C@@H]([C@H]([C@@H](O2)OC3=C(OC4=CC(=CC(=C4C3=O)O)O)C5=CC=C(C=C5)O)O)O)O)O)O)O
C123	Isoquercitrin	C1=CC(=C(C=C1C2=C(C(=O)C3=C(C=C(C=C3O2)O)O)O[C@H]4[C@@H]([C@H]([C@H](O4)[C@@H](CO)O)O)O)O)O
C124	Quercetin-acetyl-glycoside	-
C125	Isorhamnetin-3-O-glucoside	COC1=C(C=CC(=C1)C2=C(C(=O)C3=C(C=C(C=C3O2)O)O)O[C@H]4[C@@H]([C@H]([C@@H]([C@H](O4)CO)O)O)O)O
C126	Quinic acid	-
C127	Kaempferol-acetyl-glycoside	-
C128	Quercetin	C1=CC(=C(C=C1C2=C(C(=O)C3=C(C=C(C=C3O2)O)O)O)O)O
C129	Ferulic acid	COC1=C(C=CC(=C1)/C=C/C(=O)O)O
C130	Isorhamnetin	COC1=C(C=CC(=C1)C2=C(C(=O)C3=C(C=C(C=C3O2)O)O)O)O
C131	α-Linolenic acid	-
C132	Beta-caroten	CC1=C(C(CCC1)(C)C)/C=C/C(=C/C=C/C(=C/C=C/C=C(/C=C/C=C(/C=C/C2=C(CCCC2(C)C)C)\C)\C)/C)/C
C133	Caffeic acid	C1=CC(=C(C=C1/C=C/C(=O)O)O)O
C134	Oxalate	C(=O)(C(=O)[O-])[O-]
C135	Oxalic Acid	C(=O)(C(=O)O)O
C136	Riboflavin	CC1=CC2=C(C=C1C)N(C3=NC(=O)NC(=O)C3=N2)C[C@@H]([C@@H]([C@@H](CO)O)O)O
C137	Tocopherol	CC1=C(C=C2CCC(OC2=C1C)(C)CCCC(C)CCCC(C)CCCC(C)C)O

Compound Structure Profiling

The SMILES profiles of the identified *Moringa oleifera* leaf compounds were generated using PubChem, a chemical database maintained by the National Center for Biotechnology Information (NCBI). This step aimed to obtain the Simplified Molecular-Input Line-Entry System (SMILES) representations required for subsequent in silico analyses.

Prediction of Bioactive Compound Activities from Moringa oleifera Leaves

The biological activities of bioactive compounds from *Moringa oleifera* leaves were predicted using the WAY2DRUG PASS platform, which provides two probability estimates: probability to be active (Pa) and probability to be inactive (Pi), where activities with Pa > Pi are considered biologically probable. The Pa value reflects the likelihood of a compound exhibiting a specific biological activity, with higher values indicating greater predicted activity [15]. Compounds with Pa ≥ 0.7 were considered to have a high probability of demonstrating biological activity and a higher likelihood of experimental validation, whereas compounds with lower Pa values were considered to have moderate to low predicted activity [16,17].

To evaluate the potential anti–prostate cancer effects of the identified compounds, specific parameters were applied, including tumor protein p53 (TP53) expression enhancement and androgen receptor (AR) expression inhibition. TP53 expression enhancement was selected as a primary evaluation criterion due to the critical role of p53 in regulating cell cycle progression, maintaining genomic stability, and inducing apoptosis in response to DNA damage. Functional p53 is known to suppress tumor growth in prostate cancer, while its loss or mutation is associated with treatment resistance and disease progression [20,21].

The analysis revealed that a substantial proportion of the identified compounds exhibited predicted TP53-enhancing activity. In total, 42 compounds showed strong potential as TP53 expression enhancers with Pa values greater than 0.7. Among these, the top 20 compounds with the highest Pa values were selected for further analysis. Although androgen receptor (AR) expression inhibition was initially evaluated as a selection parameter, the predicted Pa values for AR inhibition were generally lower and less consistent than those observed for TP53 expression enhancement. Therefore, TP53-enhancing activity was prioritized as the primary criterion for compound selection in subsequent analyses. These selected compounds represent the most promising candidates for subsequent target prediction and network pharmacology analysis [22]. Detailed information on these compounds is presented in Table 2 and Figure 1.

Table 2. SAR profile of TP53 expression enhancer for top 20 *Moringa oleifera* leaves bioactive compounds with Pa scores >0.7.

Code	Compound Name	TP53 Expression Enhancer	
		Pa	Pi
C121	Vitexin	0.973	0.003
C72	(2R,3S,4S)-3-[(2S,3R,4R,5S,6R)-3,4-dihydroxy-6-(hydroxymethyl)-5-[(2S,3R,4S,5R,6R)-3,4,5-trihydroxy-6-(hydroxymethyl)tetrahydropyran-2-yl]oxy-tetrahydropyran-2-yl]oxy-2-(3,4,5-trihydroxyphenyl)chromane-4,5,7-triol	0.956	0.003
C125	Astragalin Isorhamnetin-3-O-glucoside	0.963	0.003
C5	Astragalin	0.952	0.003
C114	Vicenin-2	0.951	0.003
C28	Myricetin	0.944	0.004
C130	Isorhamnetin	0.944	0.004
C109	Adenosine	0.934	0.004
C1	Kaempferol	0.931	0.004
C132	Beta-caroten	0.925	0.004
C2	Zeaxanthin	0.920	0.004
C8	Afzelin	0.919	0.004
C66	(3R)-5-[[(2R,3S,4S,5R,6S)-6-[2-(3,4-dihydroxyphenyl)-5,7-dihydroxy-4-oxo-chromen-3-yl]oxy-3,4,5-trihydroxy-tetrahydropyran-2-yl]methoxy]-3-hydroxy-3-methyl-5-oxo-pentanoic acid	0.916	0.004
C137	Tocopherol	0.911	0.005
C13	Kaempferol 3-O-[beta-glucosyl-(1→2)]-[alpha-rhamnosyl-(1→6)]-beta-glucoside-7-O-alpha-rhamnoside	0.899	0.005
C118	Rutin	0.893	0.005
C123	Isoquercitrin	0.883	0.006
C122	Kaempferol-3-O-rutinoside	0.877	0.006
C105	Guanosine	0.850	0.008
C19	Kaempferol 3-O-[alpha-rhamnosyl-(1→2)]-[alpha-rhamnosyl-(1→4)]-beta-glucoside-7-O-alpha-rhamnoside)	0.849	0.008

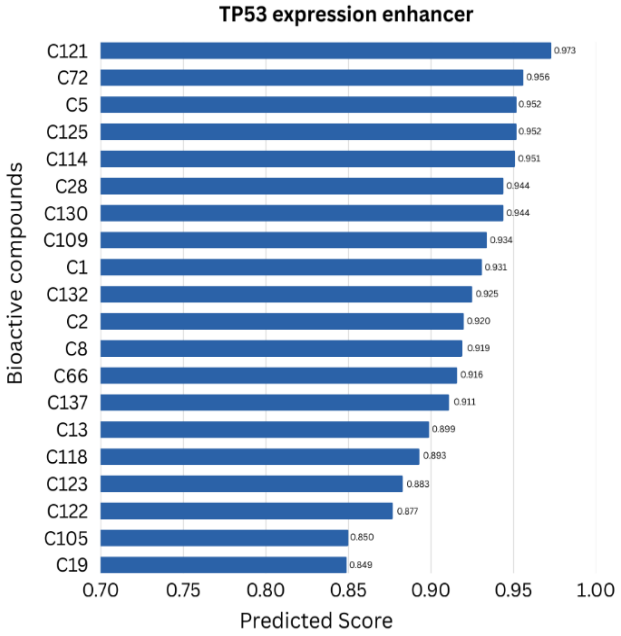

Figure 1. SAR-based prediction of TP53 expression enhancer.

Protein Target Identification and Analysis

The subsequent step involved the collection of protein target data for the 20 *Moringa oleifera* leaf compounds using the SwissTargetPrediction and Similarity Ensemble Approach (SEA) databases. The results showed that a total of 583 proteins were predicted as targets of the bioactive compounds from *Moringa oleifera* leaves. Furthermore, the search was continued to Identify proteins associated with prostate cancer using the GeneCards, GEPIA2, and OMIM databases. The results indicated that approximately 15,000 proteins were associated with prostate cancer. The protein targets of *Moringa oleifera* bioactive compounds and prostate cancer–associated proteins were mapped using the Draw Venn Diagram tool to determine overlapping protein targets. The Venn diagram results showed that 536 proteins overlapped between the protein targets of *Moringa oleifera* bioactive compounds and prostate cancer–associated proteins, as shown in Figure 2. However, this relatively large overlap may reflect not only genuine disease relevance but also the inherent bias of public databases toward well-studied and highly connected cancer-related proteins. Therefore, subsequent protein–protein interaction network construction and topological analysis were performed to prioritize biologically meaningful hub proteins rather than relying solely on the size of the overlap.

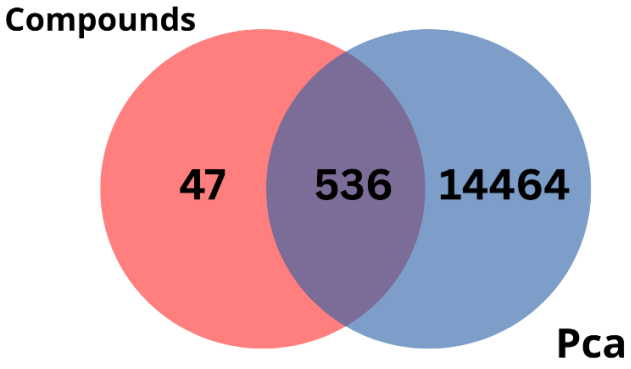

Figure 2. Intersection of target proteins associated with *Moringa oleifera* leaves compounds and prostate cancer.

The overlapping protein targets were further analyzed to identify biological pathways relevant to the protein targets of *Moringa oleifera* bioactive compounds. These overlapping targets were input into the ShinyGO platform to obtain the top 25 Kyoto Encyclopedia of Genes and Genomes (KEGG) pathway annotations. Among these 25 KEGG pathways, eight were associated with cancer-related diseases, including Epidermal Growth Factor Receptor (EGFR) tyrosine kinase inhibitor resistance, prostate cancer, the HIF-1 signaling pathway, proteoglycans in cancer, the Rap1 signaling pathway, pathways in cancer, the PI3K–Akt signaling pathway, and the MAPK signaling pathway, as shown in Figure 3.

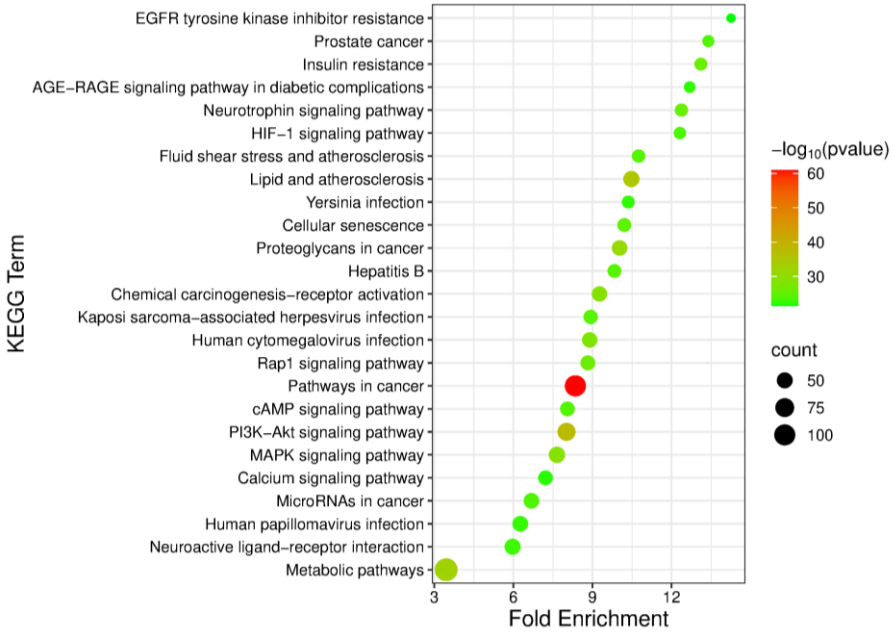

Figure 3. KEGG pathway annotation of the top 25 enriched pathways [23].

Network Pharmacology Analysis

The overlapping protein targets were imported into the STRING database and analyzed at the highest confidence level (0.900). A full STRING network was employed, and all available interaction sources were enabled, including experimental evidence, curated databases, co-expression, gene neighborhood, gene fusion, co-occurrence, and text mining. The interaction data were subsequently processed using Cytoscape for network visualization and analysis. The resulting PPI network consisted of 536 nodes and 1,394 edges. The large number of proteins increased network complexity, necessitating a more structured analytical approach to facilitate effective data management and interpretation. Network topology parameters, including degree, betweenness centrality, and closeness centrality, were applied to identify key proteins within the network. Degree represents the number of interactions between a given protein and other proteins in the network. Betweenness centrality evaluates the role of a node as a regulator of communication pathways, where nodes with high betweenness centrality values play a critical role in controlling information flow. Closeness centrality reflects the efficiency of a node in disseminating information throughout the network by considering the shortest paths to other nodes. Proteins were ranked based on degree centrality, and the top 10 proteins with the highest degree values were defined as hub proteins. Betweenness and closeness centrality were used as supporting metrics to validate the central roles of these hub proteins [24,25].

Based on these parameters, ten potential target proteins associated with the bioactive compounds of *Moringa oleifera* leaves were identified, namely ESR1, AKT1, SRC, EGFR, TP53, HSP90AA1, PIK3CA, HSP90AB1, PIK3R1, and MAPK1. The visualization of this analysis is shown in Table 3 and Figure 4, which presents a protein–protein interaction network focused

on the ten proteins with the highest degree values. Nodes with higher degree values are depicted with larger sizes and darker colors compared to nodes with lower degree values.

Table 3. Top 10 proteins based on degree scores.

Name	Degree	Betweenness Centrality	Closeness Centrality	Overall Score
ESR1	9	0.069	1.000	10.069
AKT1	8	0.058	0.900	8.958
SRC	8	0.058	0.900	8.958
EGFR	7	0.036	0.818	7.854
TP53	7	0.035	0.818	7.853
HSP90AA1	7	0.020	0.818	7.839
PIK3CA	6	0.015	0.750	6.765
HSP90AB1	6	0.008	0.750	6.758
PIK3R1	5	0.004	0.692	5.696
MAPK1	5	0.004	0.692	5.696

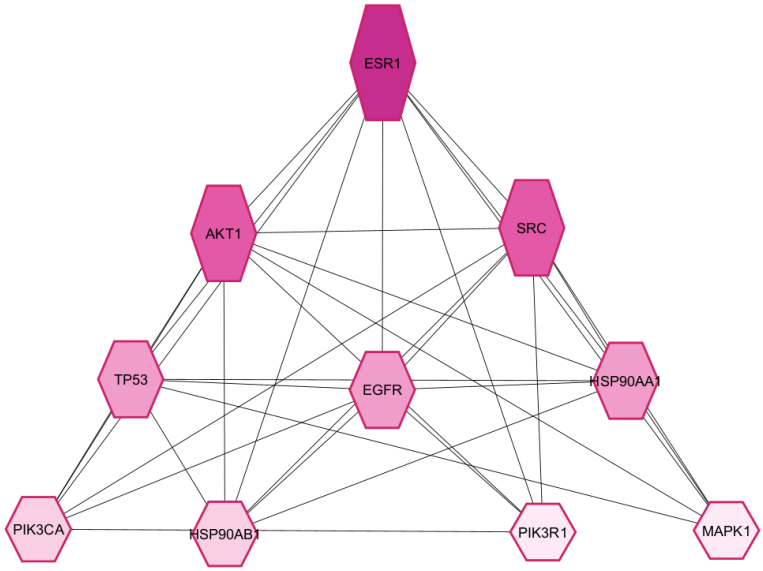

Figure 4. Protein-protein interaction network of the top 10 highest-degree proteins visualized using Cytoscape.

Among the identified hub proteins, ESR1 showed the highest degree value in the PPI network. ESR1, which encodes estrogen receptor alpha (ERα), has been shown to be expressed in prostate cancer cells and to mediate oncogenic effects of estrogen signaling, including increased tumor aggressiveness and metastasis in *in vivo* models. Notably, pharmacologic inhibition or genetic knockdown of ERα reduced osteoblastic lesion formation and lung metastasis, indicating that estrogen/ERα signaling may contribute to prostate cancer progression. Given the prominent role of ESR1 as the highest-degree hub protein and its established involvement in estrogen-driven oncogenic signaling, estrogen receptor–targeting strategies warrant consideration in the context of prostate cancer [26].

AKT1 is a central effector of the PI3K/AKT/mTOR signaling pathway, which is frequently dysregulated in prostate cancer, particularly through loss of PTEN function. Aberrant activation of AKT1 promotes tumor cell survival, proliferation, and resistance to apoptosis. Recent studies have demonstrated that alterations in the PI3K/AKT/mTOR pathway are highly prevalent in metastatic prostate cancer and are strongly associated with poor clinical outcomes and progression toward castration-resistant prostate cancer (CRPC), underscoring the critical role of AKT1 as a driver of advanced disease [27].

EGFR (epidermal growth factor receptor) is a transmembrane receptor tyrosine kinase that is frequently overexpressed in prostate cancer tissues. Clinical and experimental evidence has shown that EGFR expression increases during tumor progression, correlates with higher Gleason scores, androgen-independent growth, and poorer disease-free survival. EGFR overexpression is also enriched in circulating tumor cells and bone metastases, indicating its role in promoting migration and dissemination of prostate cancer cells. These findings suggest that EGFR signaling contributes directly to tumor aggressiveness and may represent a viable therapeutic target in advanced stages of the disease [28,29].

TP53 is a critical tumor suppressor gene that regulates cell cycle arrest, DNA repair, and apoptosis. Mutations or functional loss of TP53 are frequently observed in advanced and metastatic prostate cancer and are strongly associated with genomic instability, aggressive tumor behavior, and resistance to systemic therapies. Emerging evidence indicates that TP53 alterations have significant prognostic value and play an important role in the transition to CRPC, supporting its identification as a key hub gene within prostate cancer molecular networks [20].

Several of the top ten high-degree proteins are involved in the EGFR tyrosine kinase inhibitor resistance pathway, as shown in Figure 5. Under normal conditions, EGFR transmits growth signals upon activation by ligands such as epidermal growth factor (EGF) or transforming growth factor-α (TGF-α). When EGFR signaling is inhibited by targeted therapies, such as gefitinib or erlotinib, cancer cells may activate alternative bypass pathways to maintain survival. One such mechanism involves the activation of SRC, which subsequently stimulates the JAK–STAT signaling pathway, particularly STAT3. As illustrated in the pathway diagram, STAT3 undergoes phosphorylation, dimerization, and nuclear translocation, where activated STAT3 dimers induce the expression of genes that promote cell proliferation, survival, and angiogenesis [30].

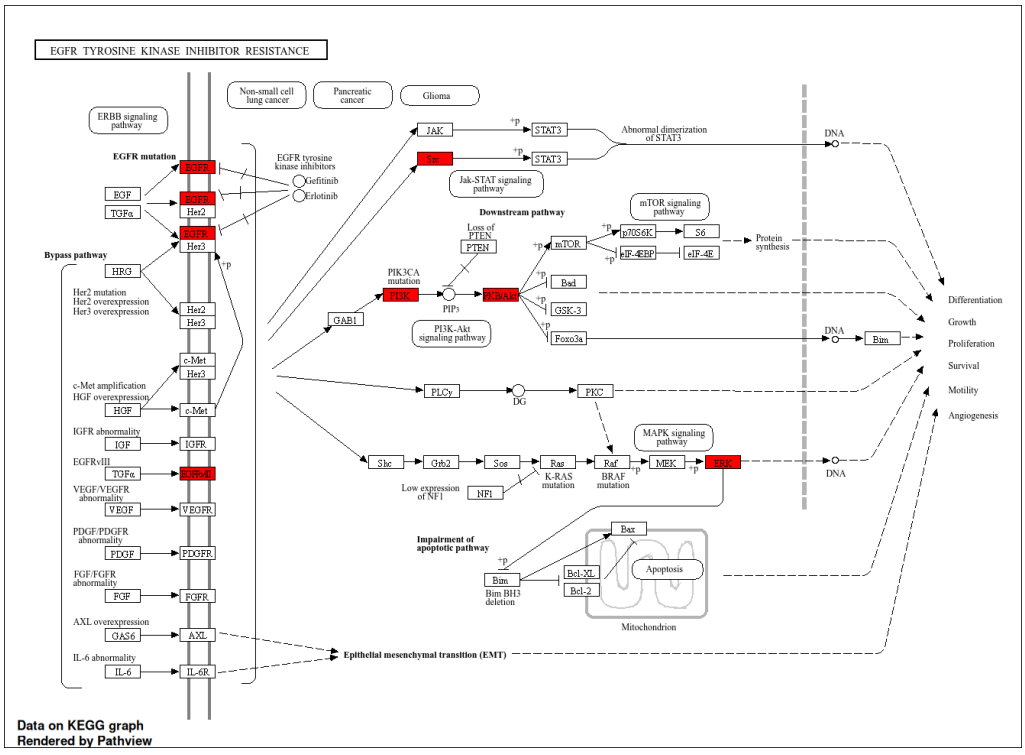

Figure 5. KEGG pathway of resistance to EGFR tyrosine kinase inhibitors [23].

In addition, PIK3CA enhances the production of phosphatidylinositol-3,4,5-trisphosphate (PIP3), leading to the activation of AKT1, a key regulator of cell survival. Activated AKT1

suppresses pro-apoptotic proteins such as Bad, inhibits the transcription factor FoxO3a, and activates the mTOR complex, thereby promoting protein synthesis and cell growth. Sustained activation of the PI3K–AKT–mTOR signaling pathway results in multiple biological effects depicted in the KEGG pathway map, including increased differentiation, growth, proliferation, motility, cell survival, and angiogenesis. Consequently, cancer cells can continue to proliferate despite EGFR inhibition by therapy [30,31]. Therefore, the identification of this pathway should be interpreted as exploratory and mechanistic, highlighting potential signaling vulnerabilities rather than immediately translatable clinical targets.

Current standard therapies for prostate cancer primarily target the androgen receptor (AR) signaling axis or microtubule dynamics, as exemplified by enzalutamide and docetaxel, respectively. However, disease progression and therapeutic resistance, particularly in advanced prostate cancer and castration-resistant prostate cancer (CRPC), are frequently associated with activation of non-AR–dependent signaling pathways. Crosstalk between AR signaling and the PI3K–AKT–mTOR pathway has been widely reported, whereby activation of PI3K–AKT signaling may function as a compensatory mechanism that contributes to reduced responsiveness to AR-targeted therapies, including enzalutamide [32,33].

In this context, the hub targets and enriched signaling pathways identified in the present study, including the EGFR tyrosine kinase inhibitor resistance pathway, should not be interpreted as direct analogs of currently approved drug targets for prostate cancer. Rather, existing evidence indicates that elevated EGFR expression is associated with a pro-migratory and pro-metastatic phenotype, shorter metastasis-free survival, and poorer overall prognosis in prostate cancer. These observations suggest that EGFR-related signaling may contribute to tumor progression and dissemination rather than representing an established therapeutic target [28]. In contrast, the PI3K–AKT–mTOR pathway is frequently dysregulated in prostate cancer and has been extensively investigated as a potential therapeutic target due to its central role in tumor cell survival, growth, and resistance to therapy [34].

Figure 6. Network visualization of bioactive compounds targeting the top 10 proteins.

Based on the interaction network analysis presented in Figure 6, bioactive compounds derived from *Moringa oleifera* leaves do not act on a single molecular target but instead exhibit multitarget activity by concurrently modulating multiple key proteins within oncogenic signaling networks. For example, kaempferol has been widely reported to possess anticancer properties through its ability to regulate multiple cell signaling pathways, in addition to inducing apoptosis

and cell cycle arrest in cancer cells. These effects are associated with the activation of tumor suppressor genes, inhibition of angiogenesis, and modulation of key signaling pathways and regulators, including PI3K/AKT, STAT3, transcription factor AP-1, Nrf2, and other cancer-related signaling molecules [35].

Considering that dysregulation of the PI3K–AKT–mTOR axis is a well-established feature of prostate cancer biology [34], targets associated with kaempferol may have potential mechanistic relevance to signaling processes implicated in prostate cancer progression. However, these observations should be regarded as exploratory and hypothesis-generating, providing mechanistic context rather than evidence of clinical efficacy or a replacement for established therapies.

Pharmacokinetic and Toxicity Evaluation

ADMETLab 3.0 was used to analyze the absorption, distribution, metabolism, excretion, and toxicity (ADMET) properties of the compounds and to evaluate their compliance with Lipinski's Rule of Five (Ro5). Lipinski's Rule of Five includes a molecular weight ≤ 500 Da, logP ≤ 5, no more than five hydrogen bond donors, and no more than ten hydrogen bond acceptors. The ADMETLab 3.0 results are presented in Table 4 and Figure 7, where the green bars indicate that compounds C121, C28, C130, C109, C1, C8, C137, and C105 comply with Ro5 criteria and exhibit favorable drug-likeness properties [36].

Table 4. Results of ADMET and drug-likeness analysis for potential compounds from *Moringa oleifera* leaves.

Compound	Pgp-inhibitor	Pgp-substrate	F20%	F30%	Bloo-Brain Barrier	H-HT	DILI	FDAMDD	Lipinski's Rule (Ro5)
C121	1.42E-06	0.419	0.360	0.991	0.021	0.575	0.934	0.226	Accepted
C72	1.66E-08	0.771	0.974	1.000	0.000	0.405	0.583	0.014	Rejected
C5	2.42E-04	0.344	0.029	0.951	0.001	0.625	0.885	0.885	Rejected
C125	2.85E-03	0.221	0.038	0.981	0.000	0.606	0.884	0.160	Rejected
C114	5.31E-10	0.661	0.454	0.999	0.003	0.655	0.960	0.019	Rejected
C28	2.05E-02	0.135	0.560	0.993	0.000	0.325	0.839	0.864	Accepted
C130	7.90E-01	0.095	0.050	0.838	0.000	0.383	0.725	0.740	Accepted
C109	5.76E-05	0.391	0.281	0.979	0.653	0.810	0.951	0.142	Accepted
C1	1.42E-01	0.163	0.084	0.716	0.001	0.386	0.703	0.805	Accepted
C132	1.15E-01	0.705	0.000	0.003	0.000	0.570	0.255	0.906	Rejected
C2	5.85E-02	0.998	0.666	0.710	0.000	0.487	0.301	0.925	Rejected
C8	6.94E-05	0.693	0.081	0.922	0.000	0.497	0.903	0.397	Accepted
C66	7.70E-11	0.069	0.954	0.999	0.000	0.931	0.398	0.598	Rejected
C137	2.49E-04	0.000	0.001	0.074	1.000	0.652	0.008	0.324	Accepted
C13	7.64E-10	0.997	0.009	0.878	0.000	0.373	0.965	0.005	Rejected
C118	6.22E-08	0.699	0.772	1.000	0.000	0.406	0.937	0.137	Rejected
C123	1.47E-05	0.240	0.969	1.000	0.000	0.556	0.816	0.362	Rejected
C122	5.12E-07	0.924	0.158	0.990	0.000	0.463	0.915	0.148	Rejected
C105	2.25E-05	0.553	0.027	0.942	0.348	0.927	0.997	0.092	Accepted
C19	4.42E-09	0.998	0.017	0.691	0.000	0.225	0.939	0.012	Rejected

Protox 3.0 was employed to evaluate the toxicity potential of the compounds, including the prediction of the lethal dose 50 (LD_{50}) values. The LD_{50} represents the dose of a compound that causes death in 50% of the test subjects following exposure. Toxicity categories are shown in Table 5, where higher toxicity corresponds to lower LD_{50} values, indicating that smaller doses are required to induce lethal effects. Based on the Protox 3.0 results shown in Figure 7, black dots represent compounds classified into toxicity classes V and VI, including C72, C5, C125, C130, C1, C8, C66, C137, C13, C118, C122, C123, and C19, which are considered relatively safe [36–39].

Based on the combined results from ADMETLab 3.0 and Protox 3.0, four compounds, namely C130, C1, C8, and C137 fulfilled Lipinski's Rule of Five (Ro5) criteria and exhibited relatively favorable toxicity profiles. However, these findings remain predictive in nature, and further validation through in vitro and in vivo studies is required to confirm the safety and therapeutic efficacy of the identified compounds.

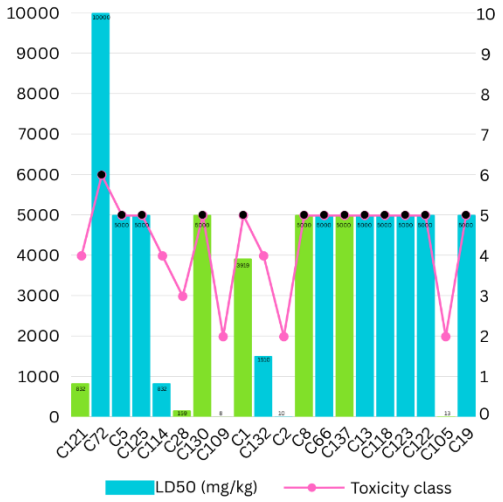

Figure 7. Prediction of toxicity based on (LD_{50}) values and toxicity classification of the compounds identified in *Moringa oleifera* leaves.

Table 5. Toxicity categories.

Class	LD_{50} (mg/kg)	Description
I	$LD_{50} < 5$	Fatal if ingested
II	$5 < LD_{50} \leq 50$	Fatal if ingested
III	$50 < LD_{50} \leq 300$	Toxic if ingested
IV	$300 < LD_{50} \leq 2000$	Harmful If ingested
V	$2000 < LD_{50} \leq 5000$	May be harmful if ingested
VI	$LD_{50} > 5000$	Non-toxic

Conclusions

This study successfully identified 137 bioactive compounds present in *Moringa oleifera* leaves, of which 20 compounds exhibited a probability of activity (Pa) greater than 0.7. These compounds were predicted to target several key proteins, including ESR1, AKT1, SRC, EGFR, TP53, HSP90AA1, PIK3CA, HSP90AB1, PIK3R1, and MAPK1. The identified target proteins are involved in multiple cancer-related signaling pathways, such as EGFR tyrosine kinase inhibitor resistance, prostate cancer, the HIF-1 signaling pathway, proteoglycans in cancer, the Rap1 signaling pathway, pathways in cancer, the PI3K–Akt signaling pathway, and the MAPK signaling pathway. The involvement of these targets in critical oncogenic pathways underscores the potential of *Moringa oleifera* leaf bioactive compounds to inhibit cancer cell progression. In addition, pharmacokinetic and toxicity evaluations revealed that four compounds (C137, C1, C8, and C130) satisfied Lipinski's Rule of Five and exhibited favorable predicted toxicity profiles, highlighting them as promising candidates for further investigation. Future experimental validation should prioritize cytotoxicity and antiproliferative assessments in widely used prostate cancer cell line models such as PC-3 and LNCaP, which represent aggressive androgen-independent and androgen-dependent prostate cancer phenotypes, respectively [40]. For in vivo validation, antitumor efficacy can be evaluated using established PC-3

xenograft mouse models as a relevant preclinical platform to assess therapeutic potential in an organismal context.

Funding: This study does not receive external funding.

Ethical Clearance: Not applicable.

Informed Consent Statement: Not applicable.

Data Availability Statement: The data presented in this study are available on request from the corresponding author. The supplementary material can be accessed at https://bit.ly/supplementarymaterialMO.

Acknowledgments: The authors express their sincere appreciation to the team and the Department of Biology, Faculty of Medicine, Sam Ratulangi University, for their support and assistance during the completion of this study.

Conflicts of Interest: All the authors declare no conflicts of interest.

References

[1] Sekhoacha M, Riet K, Motloung P, Gumenku L, Adegoke A, Mashele S. Prostate Cancer Review: Genetics, Diagnosis, Treatment Options, and Alternative Approaches. *Molecules* 2022;27:5730. https://doi.org/10.3390/molecules27175730.

[2] Bray F, Laversanne M, Sung H, Ferlay J, Siegel RL, Soerjomataram I, et al. Global Cancer Statistics 2022: GLOBOCAN Estimates of Incidence and Mortality Worldwide for 36 Cancers in 185 Countries. *CA: A Cancer Journal for Clinicians* 2024;74:229–63. https://doi.org/10.3322/caac.21834.

[3] Ferlay J, Ervik M, Lam F, Laversanne M, Colombet M, Mery L, et al. Global Cancer Observatory: Cancer Today. Lyon, France: 2024.

[4] Zhou M. High-Grade Prostatic Intraepithelial Neoplasia, PIN-like Carcinoma, Ductal Carcinoma, and Intraductal Carcinoma of the Prostate. *Modern Pathology* 2018;31:71–9. https://doi.org/10.1038/modpathol.2017.138.

[5] Bach C, Pisipati S, Daneshwar D, Wright M, Rowe E, Gillatt D, et al. The Status of Surgery in the Management of High-Risk Prostate Cancer. *Nature Reviews Urology* 2014;11:342–51. https://doi.org/10.1038/nrurol.2014.100.

[6] Safriadi F, Umbas R, Hakim L, Warli SM, Hamid AR, Hudaya S, et al. Panduan Penanganan Kanker Prostat. *Ikatan Ahli Urologi Indonesia* 2022.

[7] Okpako IO, Ng'ong'a FA, Kyama CM, Njeru SN. Network Pharmacology, Molecular Docking, and in Vitro Study on Aspilia Pluriseta against Prostate Cancer. *BMC Complementary Medicine and Therapies* 2024;24:338. https://doi.org/10.1186/s12906-024-04642-8.

[8] Abd Karim NA, Adam AHB, Jaafaru MS, Rukayadi Y, Abdull Razis AF. Apoptotic Potential of Glucomoringin Isothiocyanate (GMG-ITC) Isolated from Moringa Oleifera Lam Seeds on Human Prostate Cancer Cells (PC-3). *Molecules* 2023;28:3214. https://doi.org/10.3390/molecules28073214.

[9] Pareek A, Pant M, Gupta MM, Kashania P, Ratan Y, Jain V, et al. Moringa Oleifera: An Updated Comprehensive Review of Its Pharmacological Activities, Ethnomedicinal, Phytopharmaceutical Formulation, Clinical, Phytochemical, and Toxicological Aspects. *International Journal of Molecular Sciences* 2023;24:2098. https://doi.org/10.3390/ijms24032098.

[10] Rifa Musyaropah, Tri Cahyanto. Studi Pemanfaatan Tanaman Kelor (Moringa Oleifera) Sebagai Pengobatan Tradisional Di Kampung Cibeas Desa Cintaraja Kecamatan Singaparna Kabupaten Tasikmalaya. *Flora : Jurnal Kajian Ilmu Pertanian Dan Perkebunan* 2025;2:44–54. https://doi.org/10.62951/flora.v2i1.213.

[11] Khan F, Pandey P, Ahmad V, Upadhyay TK. Moringa Oleifera Methanolic Leaves Extract Induces Apoptosis and G0/G1 Cell Cycle Arrest via Downregulation of Hedgehog Signaling Pathway in Human Prostate PC-3 Cancer Cells. *Journal of Food Biochemistry* 2020;44. https://doi.org/10.1111/jfbc.13338.

[12] Ju J, Gothai S, Hasanpourghadi M, Nasser A, Aziz Ibrahim I, Shahzad N, et al. Anticancer Potential of Moringa Oleifera Flower Extract in Human Prostate Cancer PC-3 Cells via Induction of Apoptosis and Downregulation of AKT Pathway. *Pharmacognosy Magazine* 2018;14:477. https://doi.org/10.4103/pm.pm_516_17.

[13] Xie J, Luo F, Shi C, Jiang W, Qian Y, Yang M, et al. Moringa Oleifera Alkaloids Inhibited PC3 Cells Growth and Migration Through the COX-2 Mediated Wnt/β-Catenin Signaling Pathway. *Frontiers in Pharmacology* 2020;11. https://doi.org/10.3389/fphar.2020.523962.

[14] Noor F, Tahir ul Qamar M, Ashfaq UA, Albutti A, Alwashmi ASS, Aljasir MA. Network Pharmacology Approach for Medicinal Plants: Review and Assessment. *Pharmaceuticals* 2022;15:572. https://doi.org/10.3390/ph15050572.

[15] Patil PA, Kumbhar BV. Structure Based Drug Design and Machine Learning Approaches for Identifying Natural Inhibitors against the Human AβIII Tubulin Isotype. *Scientific Reports* 2025;15:32716. https://doi.org/10.1038/s41598-025-17708-5.

[16] Prasetyorini BE, Kusumawardani A, Fitriani F, Rachman PO, Amelinda N, Ramadhani A. Analisis In Silico Senyawa Aktif Batang Kayu Bajakah (Spatholobus Littoralis Hassk) Sebagai Terapi Psoriasis. *Herb-Medicine Journal* 2022;5:26. https://doi.org/10.30595/hmj.v5i2.12744.

[17] Kula K, Kuś E. In Silico Study About Substituent Effects, Electronic Properties, and the Biological Potential of 1,3-Butadiene Analogues. *International Journal of Molecular Sciences* 2025;26:8983. https://doi.org/10.3390/ijms26188983.

[18] Noviandy TR, Idroes GM, Mohd Fauzi F, Idroes R. Application of Ensemble Machine Learning Methods for QSAR Classification of Leukotriene A4 Hydrolase Inhibitors in Drug Discovery. *Malacca Pharmaceutics* 2024;2:68–78. https://doi.org/10.60084/mp.v2i2.217.

[19] Wang J, Du Y, Jiang L, Li J, Yu B, Ren C, et al. LC-MS/MS-Based Chemical Profiling of Water Extracts of Moringa Oleifera Leaves and Pharmacokinetics of Their Major Constituents in Rat Plasma. *Food Chemistry: X* 2024;23:101585. https://doi.org/10.1016/j.fochx.2024.101585.

[20] Ofner H, Kramer G, Shariat SF, Hassler MR. TP53 Deficiency in the Natural History of Prostate Cancer. *Cancers* 2025;17:645. https://doi.org/10.3390/cancers17040645.

[21] Quistini A, Chierigo F, Fallara G, Depalma M, Tozzi M, Maggi M, et al. Androgen Receptor Signalling in Prostate Cancer: Mechanisms of Resistance to Endocrine Therapies. *Research and Reports in Urology* 2025;Volume 17:211–23. https://doi.org/10.2147/RRU.S388265.

[22] Chappell WH, Lehmann BD, Terrian DM, Abrams SL, Steelman LS, McCubrey JA. P53 Expression Controls Prostate Cancer Sensitivity to Chemotherapy and the MDM2 Inhibitor Nutlin-3. *Cell Cycle* 2012;11:4579–88. https://doi.org/10.4161/cc.22852.

[23] Tang D, Chen M, Huang X, Zhang G, Zeng L, Zhang G, et al. SRplot: A Free Online Platform for Data Visualization and Graphing. *PLOS ONE* 2023;18:e0294236. https://doi.org/10.1371/journal.pone.0294236.

[24] Shou X, Wang Y, Zhang X, Zhang Y, Yang Y, Duan C, et al. Network Pharmacology and Molecular Docking Analysis on Molecular Mechanism of Qingzi Zhitong Decoction in the Treatment of Ulcerative Colitis. *Frontiers in Pharmacology* 2022;13. https://doi.org/10.3389/fphar.2022.727608.

[25] Tallei TE, Fatimawali, Adam AA, Ekatanti D, Celik I, Fatriani R, et al. Molecular Insights into the Anti-Inflammatory Activity of Fermented Pineapple Juice Using Multimodal Computational Studies. *Archiv Der Pharmazie* 2023. https://doi.org/10.1002/ardp.202300422.

[26] Belluti S, Imbriano C, Casarini L. Nuclear Estrogen Receptors in Prostate Cancer: From Genes to Function. *Cancers* 2023;15:4653. https://doi.org/10.3390/cancers15184653.

[27] Sutera P, Kim J, Kumar R, Deek RA, Stephenson R, Mayer T, et al. PIK3/Akt/MTOR Pathway Alterations in Metastatic Castration-sensitive Prostate Cancer. *The Prostate* 2024;84:1301–8. https://doi.org/10.1002/pros.24765.

[28] Nastały P, Stoupiec S, Popęda M, Smentoch J, Schlomm T, Morrissey C, et al. EGFR as a Stable Marker of Prostate Cancer Dissemination to Bones. *British Journal of Cancer* 2020;123:1767–74. https://doi.org/10.1038/s41416-020-01052-8.

[29] Guo R, Shi L, Chen Y, Lin C, Yin W. Exploring the Roles of NcRNAs in Prostate Cancer via the PI3K/AKT/MTOR Signaling Pathway. *Frontiers in Immunology* 2025;16. https://doi.org/10.3389/fimmu.2025.1525741.

[30] Huang L, Fu L. Mechanisms of Resistance to EGFR Tyrosine Kinase Inhibitors. *Acta Pharmaceutica Sinica B* 2015;5:390–401. https://doi.org/10.1016/j.apsb.2015.07.001.

[31] Pearson HB, Li J, Meniel VS, Fennell CM, Waring P, Montgomery KG, et al. Identification of Pik3ca Mutation as a Genetic Driver of Prostate Cancer That Cooperates with Pten Loss to Accelerate Progression and Castration-Resistant Growth. *Cancer Discovery* 2018;8:764–79. https://doi.org/10.1158/2159-8290.CD-17-0867.

[32] Adelaiye-Ogala R, Gryder BE, Nguyen YTM, Alilin AN, Grayson AR, Bajwa W, et al. Targeting the PI3K/AKT Pathway Overcomes Enzalutamide Resistance by Inhibiting Induction of the Glucocorticoid Receptor. *Molecular Cancer Therapeutics* 2020;19:1436–47. https://doi.org/10.1158/1535-7163.MCT-19-0936.

[33] Tortorella E, Giantulli S, Sciarra A, Silvestri I. AR and PI3K/AKT in Prostate Cancer: A Tale of Two Interconnected Pathways. *International Journal of Molecular Sciences* 2023;24:2046. https://doi.org/10.3390/ijms24032046.

[34] Hashemi M, Taheriazam A, Daneii P, Hassanpour A, Kakavand A, Rezaei S, et al. Targeting PI3K/Akt Signaling in Prostate Cancer Therapy. *Journal of Cell Communication and Signaling* 2023;17:423–43. https://doi.org/10.1007/s12079-022-00702-1.

[35] Almatroudi A, Allemailem KS, Alwanian WM, Alharbi BF, Alrumaihi F, Khan AA, et al. Effects and Mechanisms of Kaempferol in the Management of Cancers through Modulation of Inflammation and Signal Transduction Pathways. *International Journal of Molecular Sciences* 2023;24:8630. https://doi.org/10.3390/ijms24108630.

[36] Bickerton GR, Paolini G V, Besnard J, Muresan S, Hopkins AL. Quantifying the Chemical Beauty of Drugs. *Nature Chemistry* 2012;4:90–8. https://doi.org/10.1038/nchem.1243.

[37] Nursanti O, Wardani I, Hadisoebroto G. Validasi Penambatan Molekuler (Docking) (Zingiber Officinale) Dan (Cymbopogon Citratus) Sebagai Ligan Aktif Reseptor Pparγ. *Jurnal Farmasi Higea* 2022;14:79. https://doi.org/10.52689/higea.v14i1.469.

[38] Tania AD, Kalalo MJ, Kepel BJ, Niode NJ, Kusumawaty D, Idroes R. Evaluation of the Potential for Immunomodulatory and Anti-Inflammatory Properties of Phytoconstituents Derived from Pineapple [Ananas Comosus (L.) Merr.] Peel Extract Using an In Silico Approach. *Philippine Journal of Science* 2022;151:397–410.

[39] Fatimawali, Tallei TE, Kepel BJ, Bodhi W, Manampiring AE, Nainu F. Molecular Insight into the Pharmacological Potential of Clerodendrum Minahassae Leaf Extract for Type-2 Diabetes Management Using the Network Pharmacology Approach. *Medicina* 2023;59:1899. https://doi.org/10.3390/medicina59111899.

[40] Tai S, Sun Y, Squires JM, Zhang H, Oh WK, Liang C, et al. PC3 Is a Cell Line Characteristic of Prostatic Small Cell Carcinoma. *The Prostate* 2011;71:1668–79. https://doi.org/10.1002/pros.21383.